IEEE Access
Multidisciplinary | Rapid Review | Open Access Journal

Received August 5, 2020, accepted August 30, 2020, date of publication September 7, 2020, date of current version September 21, 2020.

*Digital Object Identifier 10.1109/ACCESS.2020.3022488*

# Single-Phase Consensus-Based Control for Regulating Voltage and Sharing Unbalanced Currents in 3-Wire Isolated AC Microgrids

**CLAUDIO BURGOS-MELLADO[1], (Member, IEEE), JACQUELINE LLANOS[2], (Member, IEEE), ENRIQUE ESPINA[3], (Graduate Student Member, IEEE), DORIS SÁEZ[3,4], (Senior Member, IEEE), ROBERTO CÁRDENAS[3], (Senior Member, IEEE), MARK SUMNER[1], (Senior Member, IEEE), AND ALAN WATSON[1], (Member, IEEE)**

[1]PEMC Group, University of Nottingham, Nottingham NG7 2RD, U.K.
[2]Departamento de Eléctrica y Electrónica, Universidad de las Fuerzas Armadas ESPE, Sangolquí 171103, Ecuador
[3]Department of Electrical Engineering, University of Chile, Santiago 8370451, Chile
[4]Instituto Sistemas Complejos de Ingeniería, Santiago 8370397, Chile

Corresponding author: Claudio Burgos-Mellado (claudio.burgosmellado1@nottingham.ac.uk)

The work of Enrique Espina was supported by the Chilean National Commission for Scientific and Technological Research/Formation of Advanced Human Capital Programme (CONICYT/PFCHA)/Doctorado Nacional/2017-21171858. The work of Doris Sáez was supported in part by the National Fund for Scientific and Technological Development (FONDECYT) under Grant 1170883, in part by the National Agency of Research and Development/Associative Research Program (ANID PIA)/Basal under Grant AFB180003, and in part by the Solar Energy Research Center (SERC), Chile, under Grant ANID/FONDAP/15110019. The work of Roberto Cárdenas was supported in part by the National Agency of Research and Development (ANID)/Basal under Grant FB0008, and in part by the National Fund for Scientific and Technological Development (FONDEQUIP) under Grant EQM160122.

**ABSTRACT** A distributed control strategy is proposed to share unbalanced currents in three-phase three-wire isolated AC Microgrids (MGs). It is based on a novel approach where, rather than analysing the MG as a three-phase system, it is analysed as three single-phase subsystems. The proposal uses a modified single-phase $Q-E$ droop scheme where two additional secondary control actions are introduced per phase. The first control action performs voltage regulation, while the second one achieves the sharing of negative sequence current components between the 3-legs power converters located in the MG. These secondary control actions are calculated online using a consensus-based distributed control scheme to share negative sequence current components, voltage regulation, and regulating the imbalance at the converters' output voltage to meet the IEEE power quality standards. The proposed methodology has the following advantages over other distributed control solutions, such as those based on the symmetrical components or those based on the Conservative Power Theory: (i) it achieves sharing of unbalanced currents, inducing smaller imbalances in the converters' output voltages than those of other methods, and (ii) the sharing of the unbalanced currents is simultaneously realised in both the sequence domain and the a-b-c domain. The latter is difficult to achieve using other solutions, as will be demonstrated in this work. Extensive experimental validation of the proposed distributed approach is provided using a laboratory-scale 3-wire MG.

**INDEX TERMS** Consensus algorithm, distributed control, microgrids, unbalanced currents sharing.

## I. INTRODUCTION

An MG is inherently an unbalanced system where unbalanced loads produce negative sequence components in its currents and voltages [1], and these can cause problems in the MG. For example, negative sequence voltage components produce oscillations in the torque of induction machines and synchronous generators [2]. This, in turn, may reduce the efficiency and useful life of these machines [3], [4]. Other effects of imbalance are localised heating in machines and power converters and reduced loading capability of conventional synchronous generators [4], [5]. Unbalanced currents can create other issues. For example, if the voltages at the output of the power converters in an AC MG are balanced, then the currents contain both positive and negative sequence components. In this case, the line current or the converter's output current could have a significantly higher peak in one phase than the other phases at a particular operating point. As a consequence, the total power output from that converter could be limited below its rated value. This situation seriously

The associate editor coordinating the review of this manuscript and approving it for publication was Jahangir Hossain.

deteriorate if the overcurrent protection of that converter is activated, and thus, it is disconnected from the MG. To avoid that, control schemes for sharing the negative sequence current components among the power converters in MGs are considered very important for MGs with a relatively high level of load imbalance [6], [7].

The sharing of unbalanced currents is achieved by increasing the voltage imbalance at the output of the power converters [6]–[8]. The maximum unbalanced voltage allowed in the MG has to be regulated to avoid power quality issues as it is defined by the IEEE standard 1547-2018 [9]. Therefore, there is a trade-off between the sharing of unbalanced currents among the power converters and the voltage quality of their output voltages. The sharing of imbalance can be realised using centralised [6]–[11] and distributed control approaches. The former has been widely used to address imbalance issues, whereas recently, there has been increasing interest in the distributed approach because it has the following advantages: it has improved reliability and flexibility, is scalability and has plug-and-play operation, and has good tolerance to failures in the communication links [12]–[14]. Distributed control approaches have already been proposed for the improvement of reactive-power sharing [15], [16], to achieve simultaneously, voltage regulation and reactive-power sharing [17]–[20], the management of congestion in the distribution lines [21], optimal dispatch [13], [21], and distributed predictive controls in [22], [23] for frequency and voltage regulation.

Regarding the problem of sharing unbalanced currents, to the best of the authors' knowledge, distributed controllers have been proposed only in [24], [25] and [26]. These methods are based on the concept of the virtual impedance loop, which means that negative and/or zero sequence impedances are implemented to control the sharing of unbalanced currents between the power converters. In [24], a distributed algorithm is proposed to achieve cooperative sharing of the negative sequence currents and compensation of the voltage imbalance between two power converters. Experimental results validated the proposal. However, it is not addressed in this publication any methodology to apply the proposed control algorithm to MGs with more than two converters.

A more generalised distributed control scheme for achieving reactive and imbalance power-sharing is proposed in [25]. A consensus strategy to adaptively regulate the magnitude of both the positive and negative sequence virtual impedances is proposed. Experimental results validate the proposal. However, the method proposed in [25] does not limit imbalance in the voltages. This issue is addressed in [26], where a distributed control scheme is proposed to improve the sharing of imbalances in 4-wire MGs and, at the same time, regulate the imbalance in the voltage at the output of the power converters to meet the appropriate IEEE power quality standards. Experimental results are provided.

The distributed approaches reported in [24], [25] and [26] are based on the application of virtual impedance loops [27]; thus, they need to identify positive, negative and/or zero sequence current components. In [24], [25], this is performed using symmetrical component theory (SCT). However, algorithms to implement SCT are strongly affected by noise, harmonic distortion, variations in the sampling time, etc. [28], [29], affecting its performance [30]. This drawback is overcome in [26], where a current transform based on the Conservative Power Theory (CPT) [8] is used. However, the implementation of the CPT algorithm represents a relatively high computational burden for the control platform [31]. Therefore, more advanced capable controllers are required, increasing the cost of this solution.

In [24]–[26], the sharing of imbalance is achieved, controlling the magnitude of the negative sequence current supplied by the converters, but not its negative sequence phase angle. Therefore, when consensus is achieved, and all the converters are supplying the same magnitude of negative sequence currents to the load, it does not mean that in the a-b-c domain the magnitude of the current in phase "a" of one converter is similar or equal to the current supplied on phase "a" of another converter (the same happens in phases "b" and "c"). This difference is produced because regulation of only the magnitude of the negative sequence phasor in each converter, but without considering the phase angle in the regulation, is not sufficient to obtain the same current in each phase of the natural a-b-c frame. Therefore, methods reported in [24]–[26] can achieve good performance in sharing the magnitude of the negative sequence domain but not in the a-b-c domain, i.e., the magnitude of $|i_a|$ supplied to the unbalanced load by the $i^{th}$ converter could be very different to that supplied by the $h^{th}$ converter. This issue is discussed in more depth in section III-A.

To avoid these drawbacks, in this paper, a new approach is proposed where a 3-phase, 3-wire system is analysed from a single-phase point of view: instead of implementing a single three-phase $Q-E$ droop controller in the control system of the 3-leg power converters, three single-phase $Q-E$ controllers are proposed. Each of them is augmented by two additional control actions, which are generated in the secondary control level of the MG (by a novel consensus algorithm) to achieve voltage regulation and the sharing of unbalanced currents. The main characteristics of the proposal are (i) simplicity, since it does not require a high computational capability, and (ii) robustness since it avoids the use of sequence component identification algorithms. The contributions of this work are:

- To the best of the authors' knowledge, this is the first paper to propose, demonstrate and validate that the sharing of negative sequence current components in 3-leg converters placed in a three-phase 3-wire isolated AC MGs can be advantageously controlled by using a single-phase approach. A mathematical framework of the proposed single-phase approach is provided, and it is demonstrated that the control algorithm is equivalent to regulating the negative sequence component of the current without requiring any sequence decomposition

algorithm. Extensive simulation and experimental work are provided to validate the proposal.

- The proposed distributed control scheme achieves the sharing of unbalanced currents in both the sequence domain and the a-b-c domain. This is difficult to achieve for the methods reported in [24]–[26] as will be shown in section III-A, where these methods are compared with the one proposed here. To the best of the authors' knowledge, this is the first paper, which achieves the aim of sharing imbalance in the a-b-c and sequence component domains simultaneously.
- The proposed distributed control approach achieves the sharing of unbalanced current producing smaller imbalances in the converters' output voltages than the methods based on the virtual impedance loop [24]–[26]. (See section III-A)

The rest of this paper is organised as follows: in section II, the proposed consensus algorithm and its implementation are discussed. Section III presents the simulation results, and section IV provides extensive experimental work performed to validate the proposal. Finally, section V presents the conclusions of this work.

## II. PROPOSED SINGLE-PHASE Q-E DROOP CONTROLLER

Assuming that the $i^{th}$ 3-leg droop-controlled power converter shown in FIGURE. 1, is part of a three-phase three-wire isolated AC MG. $E^*_{iabc}$ can be calculated using the $P-\omega$ and $Q-E$ droop controllers shown by (1) and (2), where $m_i$ and $n_i$ are the frequency and voltage droop coefficients, and $\omega_n$ and $E_n$ are, respectively, the nominal frequency and voltage of the MG [7], [11]. Also, the relationship between the frequency $\omega_i$ and the angle $\theta_i$ in that power converter is shown in (3).

$$\omega^*_i = \omega_n - m_i P_i \tag{1}$$

$$E^*_i = E_n - n_i Q_i \tag{2}$$

$$\theta_i = \int (\omega_n - m_i P_i)\, dt = (\omega_n - m_i P_i) \cdot t + \varphi_i \tag{3}$$

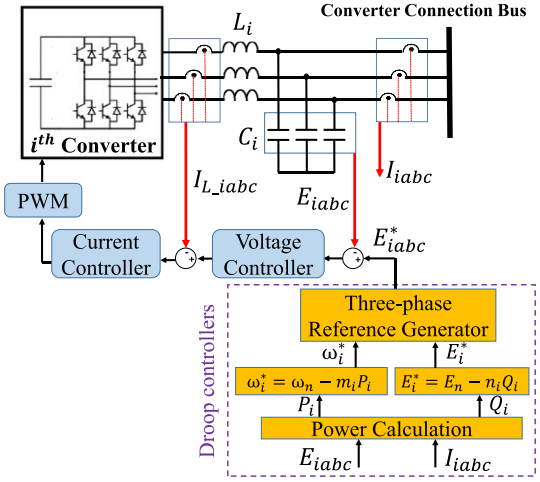


**FIGURE 1.** Typical 3-leg Droop-controlled power converter.

If the control system of the converter is working correctly, it can be assumed that $E_{iabc} \approx E^*_{iabc}$. In this case, the frequency of the voltage across the capacitor ($E_{iabc}$) will be $\omega_i$ and its magnitude will be $E_i$ [see (1) and (2) respectively].

Using (1)-(3), and assuming that $E_{iabc} \approx E^*_{iabc}$, $E_{iabc}$ can be calculated as shown in (4), where $Re\{\}$, represents the real part of the function and $j$ corresponds to the imaginary part. Based on (4), the phasor representation of $E_{iabc}$ can be calculated, as shown in (5). Based on (4)-(5), the following can be concluded: if the standard droop controllers (1)-(2) are used for controlling the $i^{th}$ power converter, balanced voltages are synthesised in its output ($E_{iabc}$). However, as was discussed at the introductory part of this paper, the sharing of unbalanced currents among the power converters is achieved by producing small imbalances in their output voltages, i.e., in $E_{iabc}$ (see FIGURE. 1).

$$E_{iabc} = \begin{pmatrix} E_{ia} \\ E_{ib} \\ E_{ic} \end{pmatrix} = \begin{pmatrix} Re\left\{E_i \cdot e^{j\varphi_i} \cdot e^{j\omega_i t}\right\} \\ Re\left\{E_i \cdot e^{j(\varphi_i - 2\pi/3)} \cdot e^{j\omega_i t}\right\} \\ Re\left\{E_i \cdot e^{j(\varphi_i + 2\pi/3)} \cdot e^{j\omega_i t}\right\} \end{pmatrix} \tag{4}$$

$$\begin{pmatrix} |E_{ia}|\angle E_{ia} \\ |E_{ib}|\angle E_{ib} \\ |E_{ic}|\angle E_{ic} \end{pmatrix} = \begin{pmatrix} E_i \cdot e^{j\varphi_i} \\ E_i \cdot e^{j(\varphi_i - 2\pi/3)} \\ E_i \cdot e^{j(\varphi_i + 2\pi/3)} \end{pmatrix} \tag{5}$$

All previously published distributed control schemes dealing with the problem of unbalanced-current sharing [24]–[26], utilises the virtual impedance loop method, usually requiring sequence component decomposition of the output currents. As aforementioned, this methodology regulates the magnitude of the negative sequence components without ensuring the sharing of imbalances in the natural a-b-c coordinates.

In this paper, voltage imbalances are created using a different approach. Therefore, it is proposed and shown in this work, that it is simple and effective to induce imbalances in $E_{iabc}$ (thus to achieve the unbalanced-current sharing) by analysing the system as three single-phase subsystems, thus, avoiding the use of (for instance) the SCT or the CPT. To do that, the single-phase $Q-E$ droop control given by (6) is proposed. In it, $\beta_i$ is a control action to achieve voltage regulation and the control actions $\beta_{ia}$, $\beta_{ib}$ and $\beta_{ic}$ are defined to achieve the sharing of unbalanced currents among the power converters in the MG. These control actions are calculated online using the proposed single-phase consensus algorithm, which will be introduced in section II-B. In (6), $Q_{ia}$, $Q_{ib}$ and $Q_{ic}$ correspond respectively to the single-phase reactive powers in phases a, b and c. To achieve the active power-sharing, the standard three-phase $P-\omega$ droop control given by (1) is used. The latter means that voltages $E^*_{ia}$, $E^*_{ib}$, $E^*_{ic}$ have the same frequency. Summarising, in this paper, it is proposed to modify the magnitude of $E^*_{ia}$, $E^*_{ib}$, $E^*_{ic}$ (see FIGURE. 1) by using (6), whereas their frequency is given by (1), meaning that the frequency is the same for all the outputs. Single-phase $P-\omega$ droop controllers are not proposed in this work since their implementation produce different frequencies in the voltages $E^*_{ia}$, $E^*_{ib}$, $E^*_{ic}$ as is discussed in [10]. In this reference, a centralised approach to achieving power-sharing per phase

is proposed. In its implementation, each phase produces different frequencies on the phase voltages during the transient response, which is adequate for some loads, for instance, heating, illumination and individual households. However, different frequencies could be a severe drawback if the microgrid is feeding three-phase loads such as motors [10].

$$\begin{aligned} E^*_{ia} &= E_n - n_i Q_{ia} + \beta_i + \beta_{ia} \\ E^*_{ib} &= E_n - n_i Q_{ib} + \beta_i + \beta_{ib} \\ E^*_{ic} &= E_n - n_i Q_{ic} + \beta_i + \beta_{ic} \end{aligned} \tag{6}$$

### A. RELATIONSHIP BETWEEN PROPOSED SINGLE-PHASE Q-E DROOP CONTROLLER AND POSITIVE AND NEGATIVE SEQUENCE COMPONENTS

It is assumed that the $i^{th}$ converter showed in FIGURE. 1 is working with the proposed single-phase $Q-E$ droop controller shown in (6) and with three-phase $P-\omega$ droop controller given by (1). Based on that, the phasor representation of voltages $E_{ia}$, $E_{ib}$ and $E_{ic}$ depicted in (5) is changed to that shown in (7), at the bottom of the page, (assuming that $E_{iabc} \approx E^*_{iabc}$, see FIGURE. 1). From (7) it can be concluded that the magnitude of $E_{iabc}$ can be regulated, at the phase level, through the control actions $\beta_i$, $\beta_{ia}$, $\beta_{ib}$, $\beta_{ic}$, and therefore, the sharing of unbalanced currents among power converters can be achieved using these degrees of freedom.

The phasor system depicted in (7) can be analysed using the SCT. This analysis establishes the relationship between the control actions of the proposed single-phase $Q-E$ droop controller ($\beta_i$, $\beta_{ia}$, $\beta_{ib}$, $\beta_{ic}$) and both the positive and negative sequence components of $E_{iabc}$. According to the SCT, phasors $|E_{ia}|\angle E_{ia}$, $|E_{ib}|\angle E_{ib}$ and $|E_{ic}|\angle E_{ic}$ (7) are related to the positive, negative and zero sequence phasors of $E_{iabc}$, through (8), as shown at the bottom of the page. (Where $\Omega = e^{\frac{2\pi}{3}j}$).

Evaluating (7) in (8), the magnitude of both positive and negative sequence phasors ($\left|E_i^+\right|$ and $\left|E_i^-\right|$) can be calculated as a function of the control actions of the proposed single-phase $Q-E$ droop controller ($\beta_i$, $\beta_{ia}$, $\beta_{ib}$, $\beta_{ic}$). These relationships are shown in (9) and (10), as shown at the bottom of the page, respectively. The zero sequence is not considered in this work since a 3-wire system is studied. Therefore, if zero sequence components are present in the voltages of (8) this component could be eliminated from the voltages before the modulation stages to avoid over-modulation issues.

From (9) it is concluded that the magnitude of the positive sequence voltage $\left|E_i^+\right|$ of $E_{iabc}$ (see FIGURE. 1) depends on the control actions $\beta_i$, $\beta_{ia}$, $\beta_{ib}$, $\beta_{ic}$ given by the proposed single-phase controller shown in (6). It is worth remembering that the control action $\beta_i$ is used to achieve voltage regulation, while the control actions $\beta_{ia}$, $\beta_{ib}$, $\beta_{ic}$ share unbalanced currents among the power converters. To avoid any coupling between the control action $\beta_i$ (voltage regulation) and $\beta_{ia}$, $\beta_{ib}$, $\beta_{ic}$ (unbalanced current sharing), the proposed consensus algorithm associated with them are designed with different dynamic (see section II-B). In this paper, the voltage regulation consensus controller is designed for a faster response than those associated with unbalanced-current sharing. From (10) it is concluded that the magnitude of the negative sequence component $\left|E_i^-\right|$ of the voltage $E_{iabc}$ is a function of the proposed control actions $\beta_{ia}$, $\beta_{ib}$, $\beta_{ic}$. This means that voltage regulation performed by the proposed single-phase controller (6) (by controlling $\beta_i$) does not affect the control of the negative sequence component $\left|E_i^-\right|$.

The proposed single-phase $Q-E$ droop scheme can control the magnitude of both positive and negative sequence components of the voltage at the output of the converters, through the proposed control actions $\beta_i$, $\beta_{ia}$, $\beta_{ib}$, $\beta_{ic}$. The magnitude of the positive sequence component $\left|E_i^+\right|$ of $E_{iabc}$ can be controlled mainly through $\beta_i$, while the magnitude of the negative sequence component $\left|E_i^-\right|$ can be controlled through the control terms $\beta_{ia}$, $\beta_{ib}$, $\beta_{ic}$ (6) and (10).

All the control terms defined by the proposed single-phase $Q-E$ droop controller (6) are calculated by the proposed consensus algorithms introduced in the next section.

### B. PROPOSED CONSENSUS ALGORITHM FOR THE SHARING OF IMBALANCE AND VOLTAGE REGULATION

As aforementioned, the sharing of unbalanced currents among power converters is achieved by inducing imbalance in the voltages at the output of the converters. This has been typically performed in the literature using virtual impedance loops. In this paper, a new approach is proposed to induce small unbalanced voltages at the output of the converters and therefore, to achieve the sharing of unbalanced currents.

$$\begin{pmatrix} |E_{ia}|\angle E_{ia} \\ |E_{ib}|\angle E_{ib} \\ |E_{ic}|\angle E_{ic} \end{pmatrix} = \begin{pmatrix} (E_n - n_i Q_{ia} + \beta_i + \beta_{ia}) \cdot e^{j\varphi_i} \\ (E_n - n_i Q_{ib} + \beta_i + \beta_{ib}) \cdot e^{j(\varphi_i - 2\pi/3)} \\ (E_n - n_i Q_{ic} + \beta_i + \beta_{ic}) \cdot e^{j(\varphi_i + 2\pi/3)} \end{pmatrix} \tag{7}$$

$$\begin{pmatrix} \left|E_i^0\right|\angle E_i^0 \\ \left|E_i^+\right|\angle E_i^+ \\ \left|E_i^-\right|\angle E_i^- \end{pmatrix} = \frac{1}{3}\begin{bmatrix} 1 & 1 & 1 \\ 1 & \Omega & \Omega^2 \\ 1 & \Omega^2 & \Omega \end{bmatrix} \cdot \begin{pmatrix} |E_{ia}|\angle E_{ia} \\ |E_{ib}|\angle E_{ib} \\ |E_{ic}|\angle E_{ic} \end{pmatrix} \tag{8}$$

$$\left|E_i^+\right|^2 = \frac{1}{9}[3(E_n + \beta_i) - n_i \cdot (Q_{ia} + Q_{ib} + Q_{ic}) + \beta_{ia} + \beta_{ib} + \beta_{ic}]^2 \tag{9}$$

$$\left|E_i^-\right|^2 = \frac{1}{9}\left[n_i \cdot \left(-Q_{ia} + \frac{1}{2}Q_{ib} + + \frac{1}{2}Q_{ic}\right) + \beta_{ia} - \frac{1}{2}\beta_{ib} - \frac{1}{2}\beta_{ic}\right]^2 + \frac{1}{12}\left[n_i \cdot (-Q_{ib} + Q_{ic}) + \beta_{ib} - \beta_{ic}\right]^2 \tag{10}$$

This can be achieved based on the proposed single-phase $Q-E$ droop controller shown in (6), and the proposed controller based on the consensus algorithm shown in (11). In (11), three single-phase consensus algorithms (one per phase) are proposed to control the magnitude of the negative sequence voltage $\left|E_i^-\right|$ at the output of the $i^{th}$ power converter. Each consensus algorithm depicted in (11) is in charge of controlling one of the three parameters ($\beta_{ia}$, $\beta_{ib}$, $\beta_{ic}$) defined by the proposed single-phase $Q-E$ droop controllers (6). It is worth remembering that the magnitude of the negative sequence voltage at the output of the $i^{th}$ converter can be controlled through $\beta_{ia}$, $\beta_{ib}$, $\beta_{ic}$ as was demonstrated in section II-A (10). Therefore, if power converters in the MG are controlled with the proposed single-phase $Q-E$ droop scheme, and the single-phase consensus algorithms shown in (11) are used to calculate their corresponding control actions $\beta_{ia}$, $\beta_{ib}$, $\beta_{ic}$: the sharing of unbalanced currents can be realised.

In (11), $PVUR_i$ corresponds to the Phase Voltage Unbalance Rate index [8] in the $i^{th}$ power converter, which is given by (12), and $PVUR_i^*$ is defined as the maximum unbalanced voltage that the $i^{th}$ converter can tolerate. In (11) and (13), $\mathcal{N}=\{1,\ldots,N\}$ with $N$ the number of power converters. (See section II-D)

$$\begin{aligned}
k_i^u\dot{\beta}_{ia} &= -\alpha^u max\left(0, PVUR_i - PVUR_i^*\right) \\
&\quad - \sum_{h\in\mathcal{N}(i)} a_{ih}\left(|I_{ia}| - |I_{ha}|\right) \\
k_i^u\dot{\beta}_{ib} &= -\alpha^u max(0, PVUR_i - PVUR_i^*) \\
&\quad - \sum_{h\in\mathcal{N}(i)} a_{ih}\left(|I_{ib}| - |I_{hb}|\right) \\
k_i^u\dot{\beta}_{ic} &= -\alpha^u max(0, PVUR_i - PVUR_i^*) \\
&\quad - \sum_{h\in\mathcal{N}(i)} a_{ih}\left(|I_{ic}| - |I_{hc}|\right)
\end{aligned} \tag{11}$$

$$\begin{aligned}
PVUR_i &= \frac{max\left(|E_{ia}|-\bar{E}, |E_{ib}|-\bar{E}, |E_{ic}|-\bar{E}\right)}{\bar{E}} \\
\bar{E} &= \left(|E_{ia}| + |E_{ib}| + |E_{ic}|\right)/3
\end{aligned} \tag{12}$$

It should be highlighted that the proposed single-phase consensus algorithms shown in (11) have two control terms; the first term on the right-hand-side is designed for maintaining the $PVUR_i$ within the values allowed by IEEE Std 1547-2018 [9]. The second term, in each of the proposed single-phase controllers shown in (11), are considered to weight respectively, the values of $|I_{ia}|$, $|I_{ib}|$ and $|I_{ic}|$ (magnitude of phase-currents in the $i^{th}$ converter), with the values of $|I_{ha}|$, $|I_{hb}|$ and $|I_{hc}|$ (magnitude of phase-currents in the $h^{th}$ converter), belonging to the other nodes ($h \neq i, h = 1,\ldots,N$, with $N$ being the number of converters in the MG). This ensures that the unbalanced currents are being shared among the power converters in the same proportion (per phase). If this current-sharing is achieved at the expense of increasing the $PVUR_i$ in some converters, exceeding their maximum allowed $PVUR_i^*$, then the first terms on the right-hand side of the proposed controllers (11) are automatically activated. Therefore, there is a trade-off between unbalanced current-sharing and fulfilling the PVUR requirements. In (11), $k_i^u$ is a positive control gain, which modifies the transient behaviour of the controller, terms $a_{ih}$ represent the entries of the adjacency matrix (communication network) [17], [18] (described in section II-D), $|I_{ia}|$, $|I_{ib}|$ and $|I_{ic}|$ correspond to the phase-current magnitude in phase "a", "b" and "c" respectively associated to the $i^{th}$ power converter.

Equation (13) shows the proposed consensus algorithm to regulate the voltage at the output of the power converters. The first term is designed to regulate the average voltage at the output of each converter to nominal values. The second term is introduced to achieve that $\beta_i$ converges to a unique value for all power converters, i.e. in steady-state, all the proposed single-phase $Q-E$ droop controllers are modified by the same factor $\beta_i$. The parameter $k^E$ modifies the transient behaviour of the controller, $E_n$ is the nominal voltage of the MG and $|E_{ia}|$, $|E_{ib}|$ and $|E_{ic}|$ correspond to the voltage magnitude in phase "a", "b" and "c" in the $i^{th}$ converter. As discussed in section III-A, to avoid any coupling between $\beta_i$ and the control actions $\beta_{ia}$, $\beta_{ib}$, $\beta_{ic}$ when the voltage regulation is performed, (11) and (13) are set to have different dynamic, this is made through $k_i^u$ and $k^E$ respectively.

$$\begin{aligned}
k^E\dot{\beta}_i = &-\left[\left(\frac{1}{3}(|E_{ia}| + |E_{ib}| + |E_{ic}|)\right) - E_n\right] \\
&- \sum\nolimits_{\substack{h\in\mathcal{N}(i)\\ h\neq i}} a_{ih}(\beta_i - \beta_h)
\end{aligned} \tag{13}$$

It is worth remembering that transient response of controllers (11) and (13) can be adjusted by modifying the gains $k_i^u$ and $k^E$, respectively. In this regard, these gains were tuned using the heuristic approach reported in [21], where a first approximation of the gains was obtained using the root locus method. Then, several simulations were carried out for different operating points to fine-tune the gains. Other methods for tuning the parameters of consensus algorithms are discussed in references [32]–[34].

### C. IMPLEMENTATION OF THE PROPOSED CONTROL SCHEME

FIGURE 2 shows the implementation of the proposed control scheme to achieve the sharing of unbalanced currents (negative sequence current components) and voltage regulation in three-phase three-wire isolated MGs. In this figure, three control layers are considered. In the first layer, output voltage and current control are performed. In this layer, each of the converters calculates their three-phase active power ($P_i$), and the single-phase reactive powers $Q_{ia}$, $Q_{ib}$ and $Q_{ic}$. In addition, the magnitude of the currents at its output ($|I_{ia}|$, $|I_{ib}|$ and $|I_{ic}|$) are calculated. The second layer corresponds to the standard three-phase $P-\omega$ droop controller (1) and the proposed single-phase $Q-E$ droop controller shown in (6). It is worth remembering that this layer enables the sharing of unbalanced currents among power converters (through the control actions $\beta_{ia}$, $\beta_{ib}$, $\beta_{ic}$), and the voltage regulation through

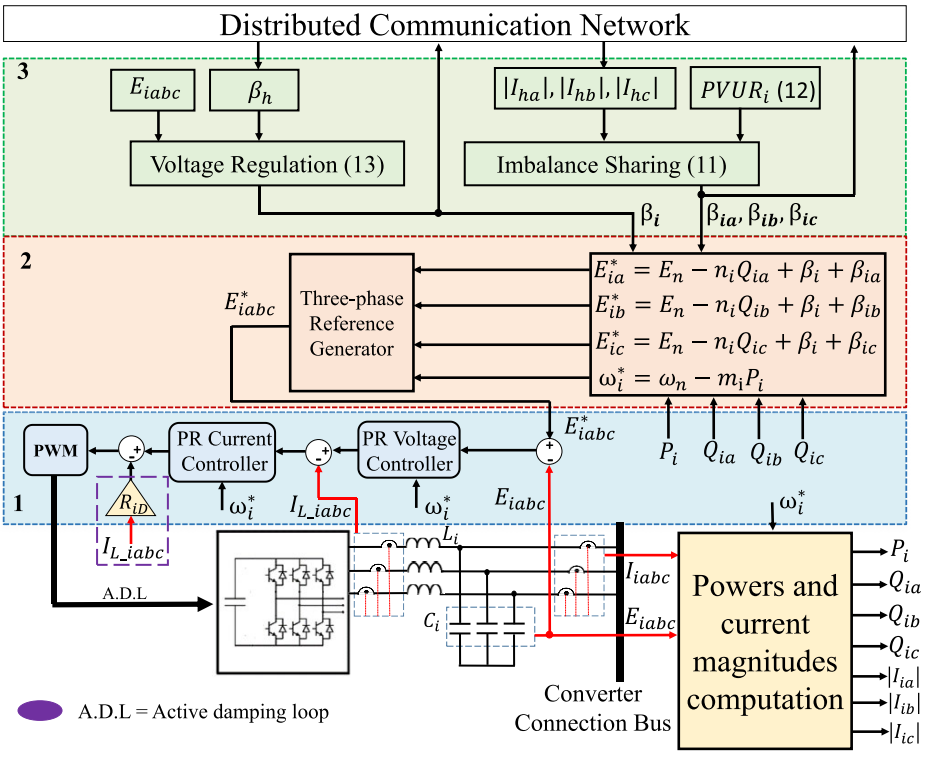


**FIGURE 2.** Proposed distributed control architecture for imbalance sharing and voltage regulation.

the control action $\beta_i$. These control actions are calculated for each power converter in the MG, in layer three, by the proposed consensus algorithms given by (11) and (13). The proposed single-phase consensus algorithms shown in (11) calculates the parameters $\beta_{ia}$, $\beta_{ib}$, $\beta_{ic}$ for each power converter, to achieve the sharing of unbalanced currents among them, and at the same time, it ensures that the voltage regulations for imbalance are met for each converter [through the first terms on the right-hand side of the controllers shown in (11)]. On the other hand, the proposed consensus algorithm depicted in (13) calculates the parameter $\beta_i$ for each power converter and, therefore, the voltage regulation is achieved. It should be highlighted that the actions $\beta_{ia}$, $\beta_{ib}$, $\beta_{ic}$ and $\beta_i$ of the proposed single-phase droop controller are modified online in the third control layer. Note that in FIGURE 2 (layer 1); an active damping loop is used (after the block labelled "PR Current Controller") for stability purposes.

FIGURE 3 shows how three-phase active power ($P_i$) is calculated by using the standard calculation in the $\alpha\beta$ reference frame. In this work, a self-tuning notch filter is used for eliminating the double frequency (of the fundamental frequency) oscillations in $P_i$. These oscillations are produced because the system is unbalanced.

FIGURE 4 shows the proposed scheme to calculate the single-phase reactive powers at the output of the $i^{th}$ power converter. In this figure, the computation of the reactive power in phase "a" is shown. From FIGURE 4, it is concluded that fictitious $\alpha\beta$ reference frames need to be defined using a

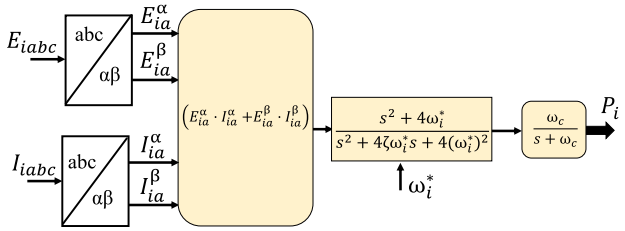


**FIGURE 3.** Computation of the three-phase active power in the $i^{th}$ power converter.

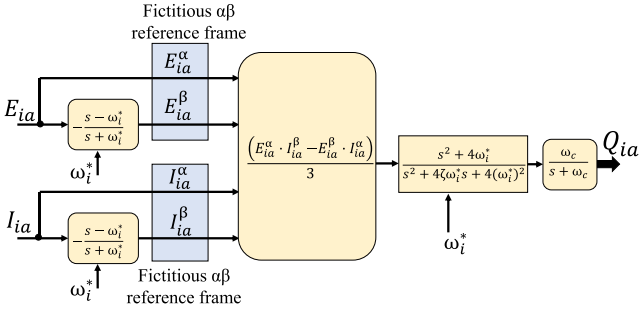


**FIGURE 4.** Computation of the single-phase reactive power in phase "a" of the $i^{th}$ power converter.

quadrature signal generator (or QSG) [10]. In these fictitious reference frames, $\alpha$ components correspond to the original signals in phase "a", i.e. $E_{ia}$ and $I_{ia}$; while the $\beta$ components are generated using QSGs. Then, the reactive power is

calculated using the standard definition for that power in the $\alpha\beta$ reference frame, and the result is divided by three. Finally, a self-tuning notch filter is used for eliminating the double frequency (of the fundamental frequency) oscillations in $Q_{ia}$. The procedure for calculating $Q_{ib}$ and $Q_{ic}$ is similar to that depicted in FIGURE 4.

Finally, FIGURE 5 shows the procedure used in this paper to calculate the magnitude of the phase-currents at the output of the converters.

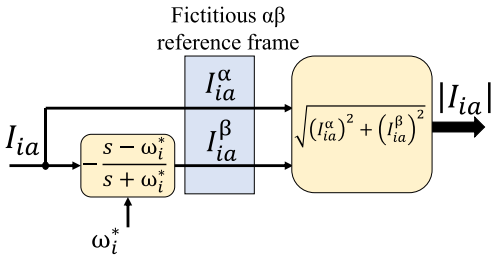


**FIGURE 5.** Computation of the magnitude of the current in phase "a" of the $i^{th}$ power converter.

Note that the proposal needs a communication network to interchange the variables $\beta_h$, $|I_{ha}|$, $|I_{hb}|$, $|I_{hc}|$, between the converters of the MG. This network is detailed in the next section.

### D. COMMUNICATION STRUCTURE

FIGURE 6 shows the three-wire MG used in this work to experimentally validate the proposed distributed control scheme. Each three-leg power converter is implemented with the control scheme shown in FIGURE 2. Moreover, the communication network considered in this work is as follows: the bidirectional network used is modelled as an undirected graph $\mathbb{G} = (\mathcal{N}, \xi, A)$ among the converters $\mathcal{N} = \{1, \ldots, N\}$, where $\xi$ is the set of communication links and $A$ is the non-negative $N \times N$ weighted adjacency matrix. The elements of $A$ are $a_{ih} = a_{hi} \geq 0$, with $a_{ih} > 0$ if and only if $\{i, h\} \in \xi$ [17].

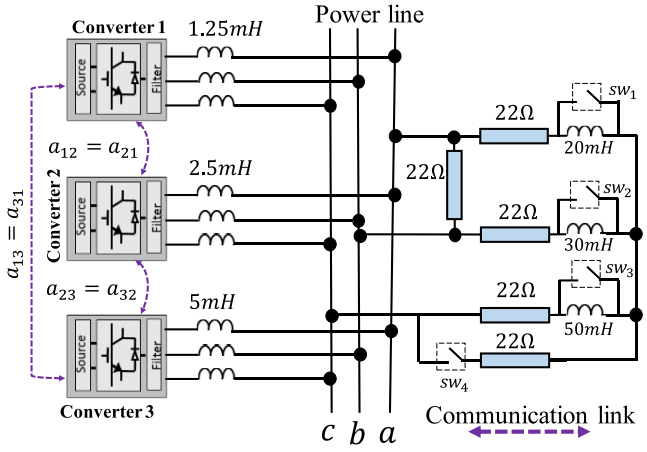


**FIGURE 6.** Microgrid and communication network considered in this work for the experimental validation.

Let $x_i \in \mathbb{R}$ denote the value of a quantity of interest at bus $i$; in this specific context, $x_i$ achieves consensus if $[x_i(t) - x_h(t)] \to 0$ as $t \to \infty$. Consensus can be achieved via the algorithm depicted in (14) [17], [18].

$$\dot{x}_i = -\sum\nolimits_{h\in\mathcal{N}(i)} a_{ij}(x_i - x_h) \tag{14}$$

According to (14), the quantities of interest are $\beta_{ia}$, $\beta_{ib}$, $\beta_{ic}$ and $\beta_i$ defined by the proposed single-phase $Q - E$ droop controller shown in (6) and the consensus of them are achieved with the proposed consensus algorithms (based on (14)) given in (11) and (13). In this work, it is assumed that the communication network allows a bidirectional exchange of information, and it is ideal, i.e., without delays. Therefore, the adjacency matrix $A$ of the system studied in this work is shown in (15). Notice that in FIGURE 6, the communication topology used in this work is depicted.

$$A = \begin{pmatrix} a_{11}=0 & a_{12}=1 & a_{13}=1 \\ a_{21}=1 & a_{22}=0 & a_{23}=1 \\ a_{31}=1 & a_{32}=1 & a_{33}=0 \end{pmatrix} \tag{15}$$

## III. SIMULATION RESULTS

In this section, the proposed distributed controller and those reported in [24]–[26] are compared. The proposed controller is also verified for the following scenarios: (i) performance considering a reactive load, and (ii) the effects of communication time delays in the communication network. These cases were not experimentally evaluated because of some experimental issues, e.g. the lack of relatively large reactive loads and the difficulty of implementing communication delays in the experimental rig. However, the performance of the proposed controller is experimentally validated for a wide range of scenarios, as shown in section IV.

The MG shown in FIGURE 6 is implemented using PLECS® software with the parameters depicted in TABLE 1 (corresponding to the MG utilised in the lab for the experimental work discussed in the next section). Each one of the power converters of FIGURE 6 is controlled using the proposed distributed control scheme shown in FIGURE 2. Moreover, the communication network used is characterised by the adjacency matrix $A$ given by (15). Note that during these tests, it is considered that the switches $sw_1 - sw_4$ depicted in FIGURE 6 are opened. The simulation tests performed in this section are shown as follows.

### A. COMPARISON WITH PREVIOUS WORKS

As discussed previously, to the authors' best knowledge, distributed control schemes have been proposed for improving the imbalance sharing among power converters placed in isolated AC MGs only in [24], [25] and [26]. The control schemes reported in those references are based on the concept of virtual impedance. In [24], [25], symmetrical component theory is used to identify both the positive and the negative sequence components of currents. By contrast, in [26], this is achieved by using CPT theory. In this section, we compare the performance of the proposed distributed controller and

**TABLE 1.** System parameters used for both the simulation and the experimental work. ([1]: converter 1, [2]: converter 2, [3]: converter 3).

| Parameter | Symbol | Value |
|---|---|---|
| Nominal frequency | $\omega_n$ | $2\pi \cdot 50$ rad/s |
| Nominal voltage | $E_n$ | $110V_{RMS}$ |
| Switching frequency | $f_m$ | 16kHz |
| DC-Link voltage | $V_{DC}$ | $720^{1,2}$V/$520^{3}$V |
| Filter inductances | $L_f$ | $0.85^{1,2}$mH/$0.80^{3}$mH |
| Filter capacitances | $C$ | $70^{1,2}\mu F$ /$20^{3}$ $\mu F$ |
| Voltage closed-loop | $k_{pV}$<br>$k_{rV}$<br>$\omega_{cV}$ | $0.16^{1,2}/0.12^{3}$<br>$30^{1,2}/20^{3}$<br>0.5rad/s |
| Current closed-loop | $k_{pI}$<br>$k_{rI}$<br>$\omega_{cI}$ | $0.8^{1,2}/0.24^{3}$<br>$1500^{1,2}/1000^{3}$<br>0.5rad/s |
| Droop coefficients | $m$<br>$n$ | $1 \cdot 10^{-4}$rad/(W·s)<br>$1 \cdot 10^{-3}$V/(Var) |
| Active damping | $R_D$ | $4^{1,2}$ Ω /$2.5^{3}$ Ω |
| Voltage control gain | $k^E$ | 1 |
| Unbalanced control gain | $k_i^u$ | 1.5 |
| PVUR limit control | $\alpha^u$ | 300 |
| PVUR set point | $PVUR^*$ | 3% |

those reported in [25] and [26]. Reference [24] is not studied because it is based on the same approach of reference [25].

Two steps are considered for comparison purposes: step 1 ($0s \leq t < 15s$), where the distributed controllers are disabled and, step 2 ($15s \leq t < 30s$) where they are enabled at 15s.

FIGURE 7 shows the results obtained from the comparative analysis. As observed in FIGURE 7(d)-(f), the three distributed controllers achieve the sharing of negative sequence current components among the converters. The sharing of unbalanced currents is achieving by inducing small imbalances in the voltage at the output of the converters. In this sense, FIGURE 7 (g)-(i), shows for each of the control schemes, the PVUR index of the voltage at the output of each converter required to achieve the unbalanced current sharing. By comparing the results shown in FIGURE 7 (g)-(h) with that reported in FIGURE 7(i), it is concluded that the proposed control scheme generates lower PVURs than those achieved by the controllers reported in [25] and [26]. This result demonstrates that the proposed controller achieves the sharing of unbalanced currents, producing smaller imbalances in the converters' output voltages than the other methods. This result is an advantage of the proposed single-phase approach over the approaches reported in [25] and [26]. Finally, from FIGURE 7(a)-(c) it can be seen that the sharing of positive sequence current components is not affected when the imbalance sharing schemes are working.

One advantage of the proposed distributed controller over those reported in [25] and [26] seen in FIGURE 7, is that even though it is defined in the a-b-c reference frame, it allows the sharing of negative sequence current components among the power converters, as was demonstrated in FIGURE 7(f). An interesting test is to evaluate the performance of the distributed controllers [25] and [26] in the opposite scenario, i.e., analyse their performance in the a-b-c reference frame. This comparison is shown in FIGURE 8, where the results of FIGURE 7 (in terms of currents) are depicted in the natural a-b-c reference frame (the controllers are activated at 15s). From this figure, it can be concluded that the phase-currents are not effectively shared by the control schemes proposed in [25] and [26]. However, the proposed single-phase approach achieves an effective current sharing by phase (i.e. phase "a" to phase "c") in the power converters. This result is interesting since it shows that imbalance sharing methods defined in the sequence components domain (such as [25] and [26]), where only the magnitude of the negative sequence is controlled do not ensure a proper phase-current sharing in the a-b-c reference frame. This is because this approach aims to achieve a consensus of only the magnitudes of the negative sequence components of currents without considering their negative sequence phase angles. Therefore, when these phasors are transformed to the a-b-c natural coordinates, they produce unequal phase-currents, as demonstrated in FIGURE 8 (in the results associated with references [25] and [26]). On the other hand, in the proposed distributed control scheme (11), imbalance sharing at the phase level is achieved, since the algorithm directly regulates the magnitude of the currents in the a-b-c natural reference frame.

In summary, from this comparison work, it is concluded that the proposed distributed control scheme achieves a superior sharing of unbalanced current (producing smaller imbalances in the converters' output voltages) compared to the methods reported in [25] and [26]. Moreover, the proposed control achieves sharing of unbalanced currents in both the sequence domain and the a-b-c domain. This is not achieved by [25] and [26] since for the cases studied in this work; they share unbalanced current only in the sequence domain and considering only the magnitude of the negative sequence current phasor.

### *B. LOAD CONSUMING BOTH ACTIVE AND REACTIVE POWERS*

In this case, the performance of the proposed distributed control scheme is evaluated, considering the unbalanced load shown in FIGURE 6. Three steps are considered: (i) step 1 ($0s \leq t < 20s$), where the proposed control scheme is not working (layer 3 of FIGURE 2 is disabled), (ii) step 2 ($20s \leq t < 40s$) where the proposed consensus algorithm [see (13)] is activated to regulate the voltage at the converters' output at $120V_{RMS}$; (iii) step 3 ($40s \leq t < 70s$) where the proposed consensus algorithm [see (11)] is activated to achieve the sharing of unbalanced currents among the power converters.

FIGURE 9 shows the performance of the proposed control scheme in terms of voltage regulation. From this figure, it is concluded that in step 2, the RMS voltage at the

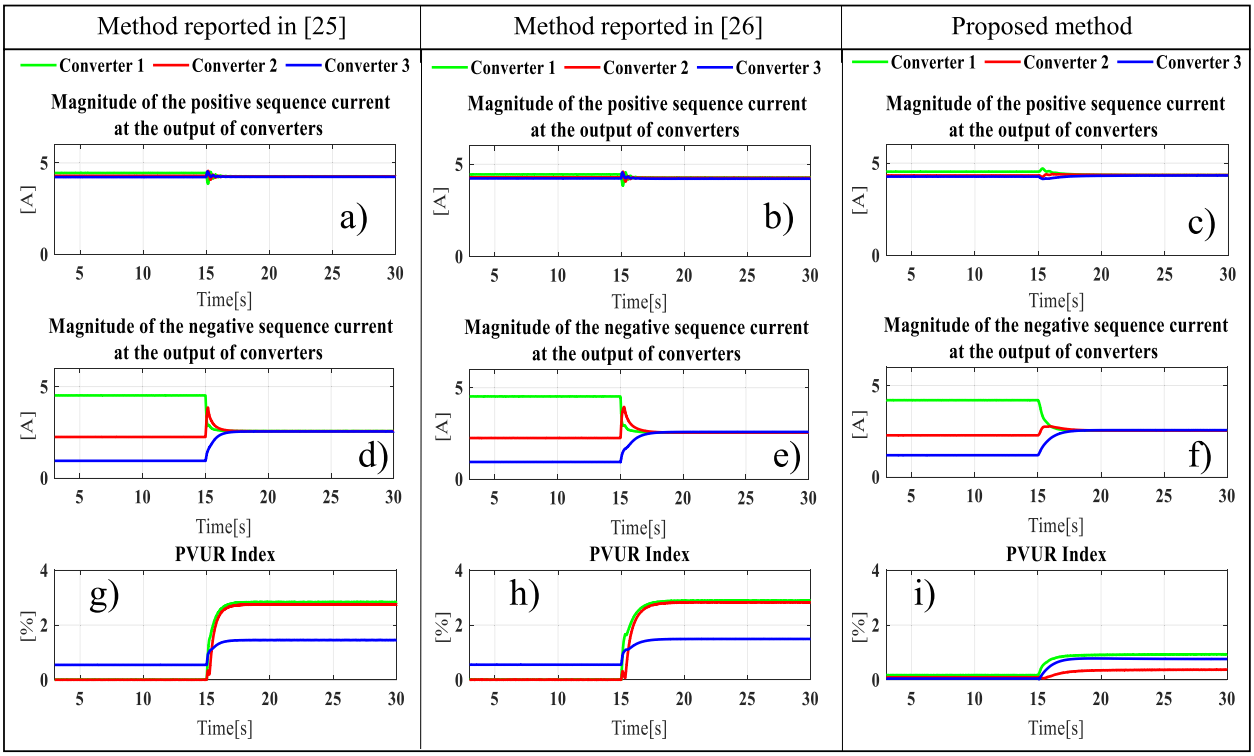


**FIGURE 7.** Comparison between the proposed distributed control scheme and those reported in references [25] and [26], (a)-(c) magnitude of the positive sequence current components at the converters' output for the three methods compared, (d)-(f) magnitude of the negative sequence current components at the converters' output for the three methods compared, (g)-(i) PVUR index of the voltage at the converters' output for the three methods compared.

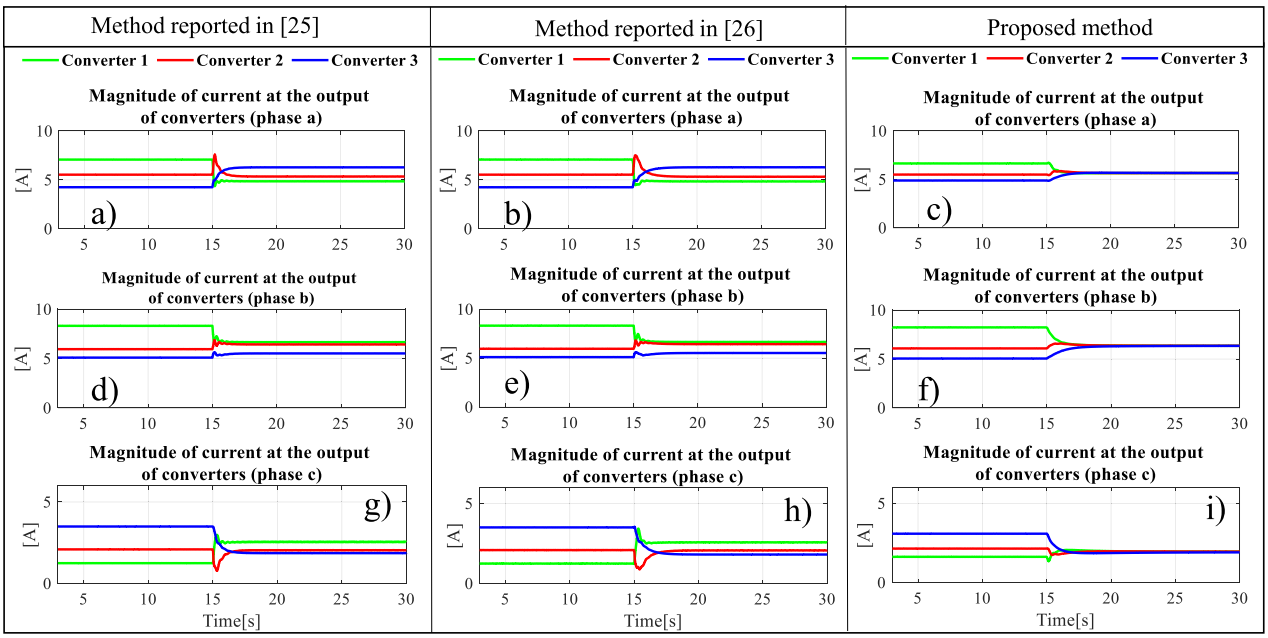


**FIGURE 8.** Comparison between the proposed distributed control scheme and those reported in references [25] and [26], (a)-(c) magnitude of the current in phase "a" at the converters' output for the three methods compared, (d)-(f) magnitude of the current in phase "b" at the converters' output for the three methods compared, (g)-(i) magnitude of the current in phase "c" at the converters' output for the three methods compared.

converters' output is effectively regulated to $120V_{RMS}$. Moreover, from t = 40s, and onwards, these voltages have some deviations due to the proposed consensus algorithm (11) is enabled to achieve the sharing of unbalanced currents, as shown in step 3 of FIGURE 10. In this figure, during step 1 and 2 [before the activation of (11)], the line currents are

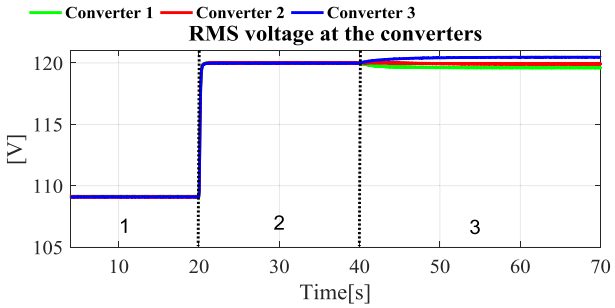


**FIGURE 9.** Average of the RMS voltage in the three phases of each power converter.

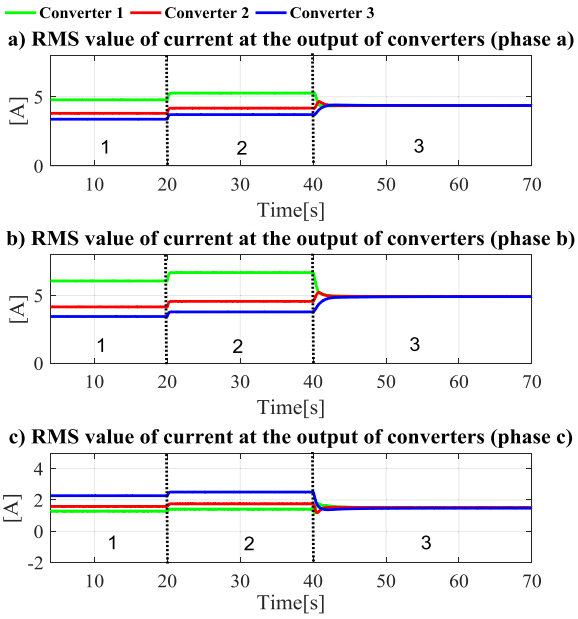


**FIGURE 10.** RMS values of currents at the converters' output.

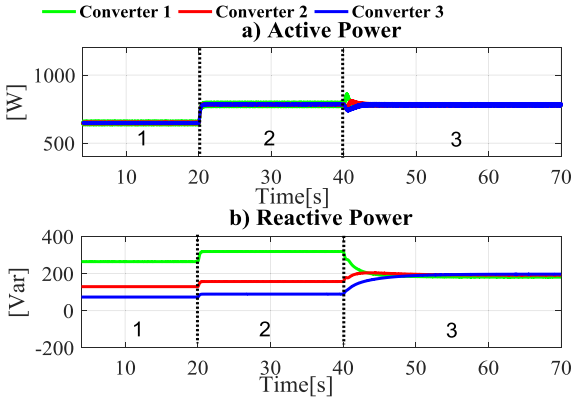


**FIGURE 11.** Three-phase active and three-phase reactive powers inject by converters to the unbalanced load.

unequally shared among the power converters due to their different line impedances (see FIGURE 6). This is corrected by the proposed control scheme, as shown in step 3 of FIGURE 10.

Finally, FIGURE 11(a) shows that the sharing of three-phase active powers is not affected by the proposed control scheme and that the sharing of the three-phase reactive power is improved when the proposed consensus algorithm of (11) is enabled [see step 3 shown in FIGURE 11(b)]. Note in FIGURE 11 that both active and reactive powers in step 2 are increased in comparison with step 1. This is because the consensus algorithm of (13) to perform voltage regulation is enabled at t = 20s, producing a power increase.

### C. EFFECTS OF TIME DELAY ISSUES

To analyse the performance of the proposed consensus algorithms, [see (11) and (13)], against communication delays, a communication time-delay $\tau$ is introduced, as shown in (16) and (17) respectively. The performance of the controllers is analysed for three cases: a) small time-delays ($\tau = 0.05$s), b) medium time-delays ($\tau = 0.5$s) and c) large time-delays ($\tau = 1$s).

$$
\begin{aligned}
k_i^u \dot{\beta}_{ia} &= -\alpha^u max\left(0, PVUR_i - PVUR_i^*\right) \\
&\quad - \sum_{h\in\mathcal{N}(i)} a_{ih}\left(|I_{ia}| - |I_{ha}(t-\tau)|\right) \\
k_i^u \dot{\beta}_{ib} &= -\alpha^u max(0, PVUR_i - PVUR_i^*) \\
&\quad - \sum_{h\in\mathcal{N}(i)} a_{ih}\left(|I_{ib}| - |I_{hb}(t-\tau)|\right) \qquad (16) \\
k_i^u \dot{\beta}_{ic} &= -\alpha^u max(0, PVUR_i - PVUR_i^*) \\
&\quad - \sum_{h\in\mathcal{N}(i)} a_{ih}\left(|I_{ic}| - |I_{hc}(t-\tau)|\right)
\end{aligned}
$$

$$
\begin{aligned}
k^E \dot{\beta}_i &= -\left[\left(\frac{1}{3}(|E_{ia}| + |E_{ib}| + |E_{ic}|)\right) - E_n\right] \\
&\quad - \sum_{\substack{h\in\mathcal{N}(i) \\ h\neq i}} a_{ih}(\beta_i - \beta_h(t-\tau)) \qquad (17)
\end{aligned}
$$

In this test, the consensus algorithms of (16) and (17) are simultaneously enabled at t = 40s, to achieve unbalanced-current sharing and voltage regulation, respectively. FIGURE 12, shows the corresponding responses for the RMS line current values at the converters' output in phases a, b and c; before and after the activation of the proposed controllers (at t = 40s). From this figure, it is concluded that consensus of these variables is achieved for all the cases considered, i.e., $\tau = 0.05$s (see FIGURE 12(a), (d) and (g)), $\tau = 0.5$s and $\tau = 1$s. Note that, for the case of large time-delays [see FIGURE 12(c), (f) and (i)], the RMS currents have some oscillations before the consensus is achieved. The same behaviour is depicted for the RMS voltages (at the converter outputs) as shown in FIGURE 13. From this test, an excellent performance of the consensus algorithms (11) and (13) is concluded, in terms of time delays.

## IV. EXPERIMENTAL VALIDATION

The MG showed in FIGURE 6. is emulated using the experimental rig depicted in FIGURE 14. Two Triphase [8] are used as 3-leg converters. Converters 1 and 2 are Triphase PM15F120 units (both operating as a 5kW converter), and

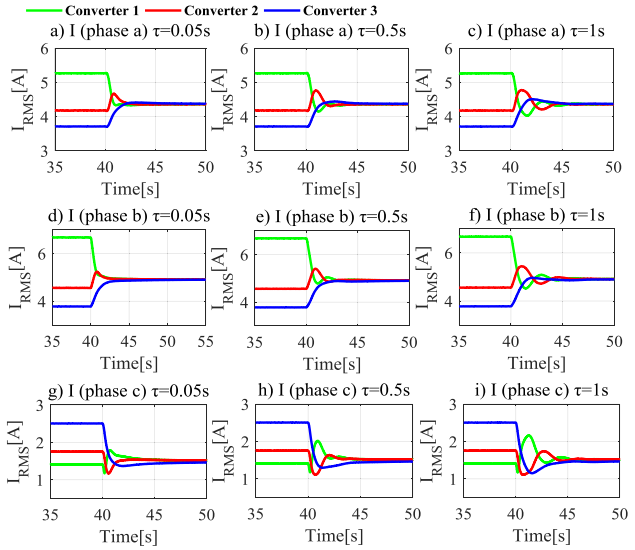


**FIGURE 12.** RMS values of currents at the converters' output considering communication delays: a) With small time-delays $\tau = 0.05$s, b) With medium time-delays $\tau = 0.5$s, c) With large time-delays $\tau = 1$s.

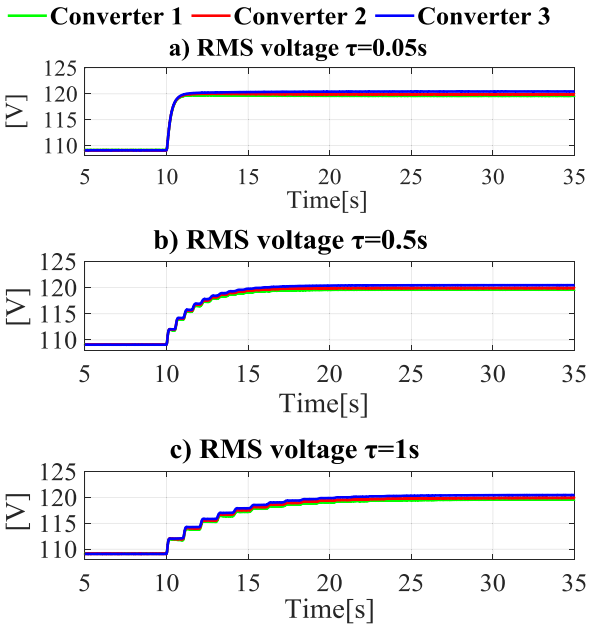


**FIGURE 13.** Average of the RMS voltage in the three phases of each power converter a) With small time-delays $\tau = 0.05$s, b) With medium time-delays $\tau = 0.5$s, c) With large time-delays $\tau = 1$s.

converter 3 is a Triphase PM5F60 (5kW) unit. The unbalanced load is implemented using resistors. In this work, the connection/disconnection of loads and generating units is realised using mechanical switches which typically produce some bouncing during connection/disconnection. The proposed distributed control scheme is implemented in the real-time target computers controlling each 3-leg power converter shown in FIGURE 14. The inner control loops are based on self-tuning voltage and current PR controllers [31]. The parameters of the experimental system and control loops are given in TABLE 1.

FIGURE 15 shows the unbalanced currents measured in the unbalanced load of the experimental MG. Because the three power converters are connected to this common load through different line inductances, the negative sequence current components injected by them into the load will be different. In this situation, and considering that the three converters have the same power rating, it is desirable that all of them inject the same amount of unbalanced currents into the system, to prevent an overload of one or more of them. In this sense, an equal distribution of unbalanced currents among the power converters is achieved by the proposed control scheme.

The experimental validation of the proposed control scheme is performed using three scenarios. Note that during this validation, it is considered that switches $sw_1 - sw_3$ are closed. (See FIGURE 6).

### A. TEST SCENARIO 1: PERFORMANCE OF THE PROPOSED CONTROL SCHEME

In this scenario, the performance of the proposed distributed scheme to achieve voltage regulation and the sharing of unbalanced currents among the power converters


**FIGURE 14.** Three-phase 3-wire isolated AC MG prototype implemented in the laboratory.

of the experimental MG is evaluated. The converters are connected to the unbalanced load through different lines impedances (see FIGURE 6). In this case, in the absence of some imbalance-sharing controller, the unbalanced currents injected are not equal: which could overload a particular converter. This situation is depicted in FIGURE 16 (step 2), where the line currents at the output of the converters are shown when the proposed imbalance-sharing controller is disabled. Indeed, in step 2 of FIGURE 16, currents injected by the converters to the load in phase "a" are similar. However, in phase "b", converter 1 injects more current than that supplied by the other power converters. Finally, in phase "c", converters 2 and 3 inject more current to the load than

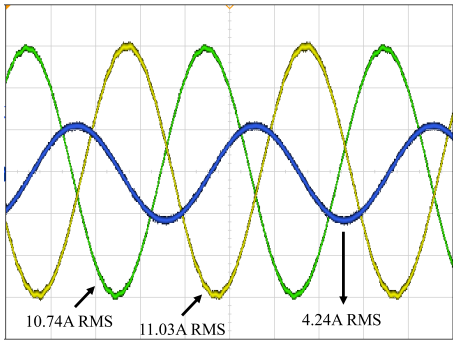


**FIGURE 15.** Currents in unbalanced load measured in the experimental rig of FIGURE 14. (5 A/div).

converter 1. In this situation (considering that the power converters have the same power rating), all of them should supply the same amount of current per phase to the unbalanced load, to prevent phase-current overloading of some converter. This is effectively achieved by the proposal as is depicted in step 3 of FIGURE 16.

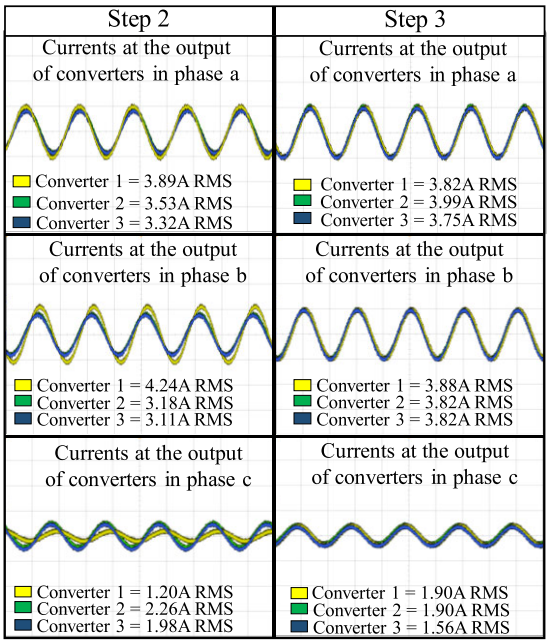


**FIGURE 16.** (Step 2) Currents injected by the power converters to the unbalanced load when the proposed control scheme is not working, (step 3) currents injected by the power converters to the unbalanced load when the proposed control scheme is working. (5 A/div).

The full test scenario discussed in this section has four steps: step 1, where the proposed control scheme is not working; step 2, where only the third control layer is activated, to achieve voltage regulation (i.e. $\beta_i$). In this step, the voltage is regulated to 120V RMS. In step 3, the proposed distributed control strategy for unbalanced-current sharing is activated (see $\beta_{ia}$, $\beta_{ib}$, $\beta_{ic}$ in FIGURE 2). Finally, in step 4, when the distributed controllers are working, an additional resistance is connected to the load (by closing switch "$sw_4$" in

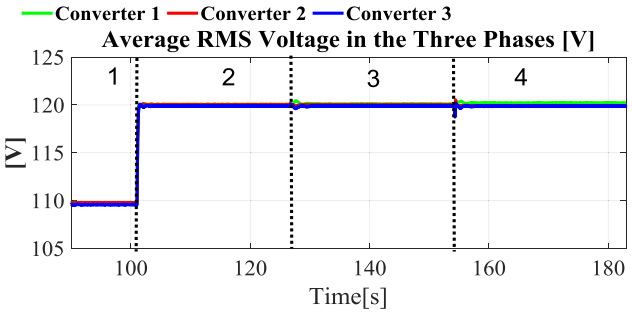


**FIGURE 17.** Average of the RMS voltage in the three phases of each power converter—MATLAB data logging of the experimental waveforms.

FIGURE 6), increasing the level of imbalance in the system. Note that $PVUR_i^* = 3\%$ is used for all the experimental tests. This meets IEEE standard 1547-2018 [9] that establish a maximum of 5% of voltage imbalances.

FIGURE 16 shows the current injected by the converters to the unbalanced load (see FIGURE 6) before (step 2) and after (step 3) the activation of the proposed control scheme for unbalanced-current sharing. From this figure, it is concluded that the proposed control scheme works very effectively.

In FIGURE 17, the voltage regulation is shown for the four steps studied. Before the activation of the proposed voltage regulation controller, the voltages at the output of the converters were close to 110V RMS. In step 2 and onwards (when the voltage regulation is enabled), voltages are regulated to 120V RMS, showing excellent performance of the proposed control scheme (13).

FIGURE 18 shows the PVUR of the voltage at the output of the converters and at the PCC during the four steps considered. In steps 3-4 (where the control scheme for the sharing of imbalance is working), the PVURs are increased a little in comparison with steps 1-2. This is because the sharing of unbalanced currents is achieved by introducing

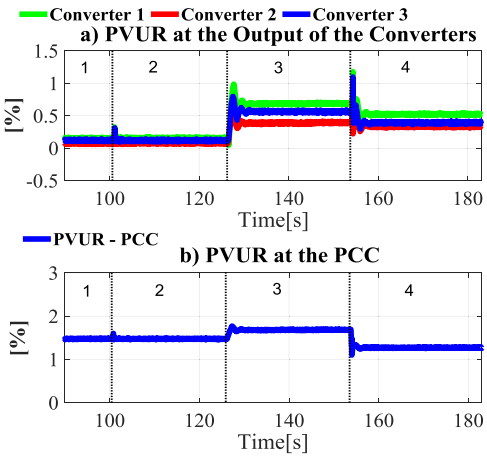


**FIGURE 18.** (a) PVUR of the voltage at the output of the converters, (b) PVUR of the voltage in the common load—MATLAB data logging of the experimental waveforms.

small imbalances in the voltage at the output of the converters, as discussed in [6], [7]. The same trend is followed by the PVUR at the PCC (see FIGURE 18(b)). In this experimental test, the control actions to limit the PVUR were not activated because the PVURs do not exceed 3% during the whole test.

Finally, FIGURE 19 shows both three-phase active and reactive powers at the output of the converters as well as the electrical frequencies. From FIGURE 19(a) it is concluded that the sharing of active power among the converters is not affected when the proposed control scheme is working (see steps 2-4 in FIGURE 19). The reactive power at the converters' output is small since the load is resistive. From FIGURE 19(c) it can be appreciated that the frequency at the output of the converters is close to the nominal value (50Hz) during the four steps studied in this experimental test.

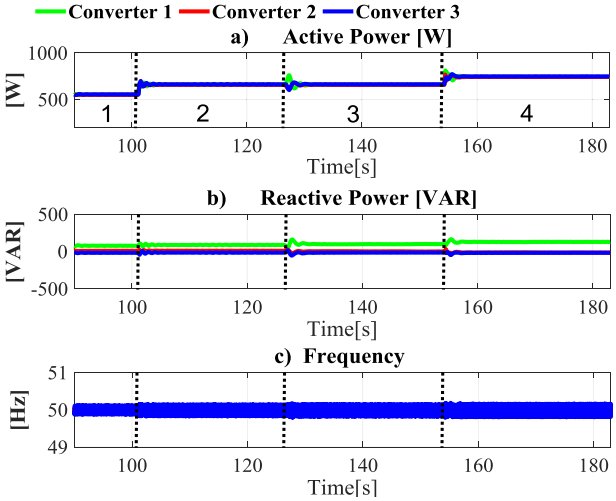


**FIGURE 19.** (a) Active power at the output of the converters, (b) Reactive powers at the output of the converters, (c) Frequency at the output of the converters—MATLAB data logging of the experimental waveforms.

### B. TEST SCENARIO 2: PLUG & PLAY OPERATION

This test shows the performance of the proposed distributed control architecture when converter 2 is disconnected and reconnected to the MG. In this experimental test, 6 steps are evaluated: step 1, where the proposed control scheme is disabled; step 2, where (13) is enabled to regulate the voltage at the output of the power converters at 120V RMS. In step 3, the distributed control systems (11) for unbalanced-current sharing are enabled (providing $\beta_{ia}$, $\beta_{ib}$, $\beta_{ic}$ for each converter). Note that in this step, the first terms on the right-hand side of (11) are not activated, and therefore, PVUR limit control is not performed. At the beginning of step 4, converter 2 is disconnected from the MG. In step 5, the PVUR limit controllers are then enabled [activating, respectively, the first terms on the right-hand side of (11)]. Finally, at the beginning of step 6, converter 2 is reconnected to the MG.

FIGURE 20 shows the current-magnitude at the output of the converters during the six steps. From step 3 and onwards, the sharing of unbalanced-currents among the converters is

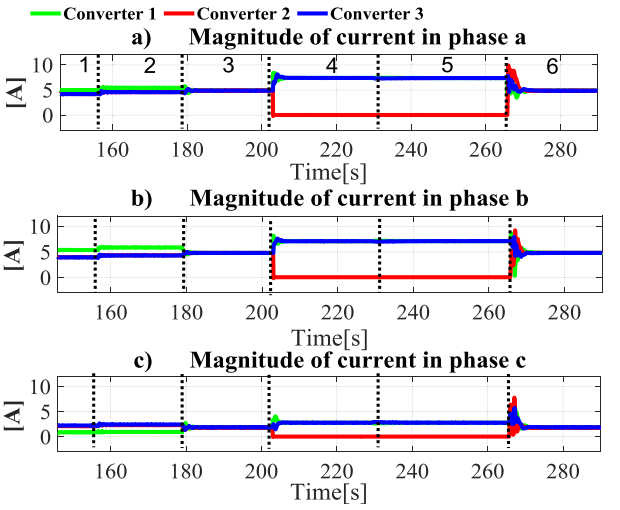


**FIGURE 20.** Magnitude of the phase-currents at the output of the converters in the 6 steps studied—MATLAB data logging of the experimental waveforms.

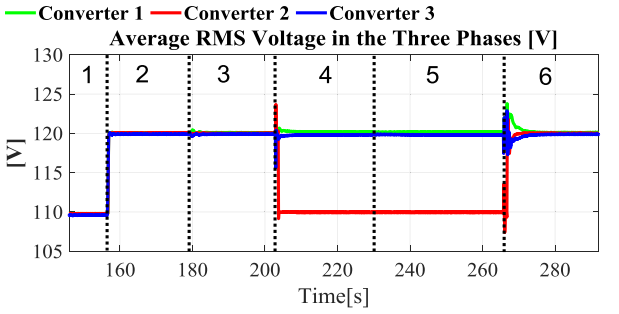


**FIGURE 21.** Average of the RMS voltage in the three phases of each power converter—MATLAB data logging of the experimental waveforms.

achieved effectively by the proposed control scheme. In particular, its robustness is demonstrated at the beginning of step 4 and at the end of step 5, where converter 2 is disconnected and reconnected to the MG, respectively. In these critical situations, the sharing of unbalanced-currents performs well after a small transient. The same behaviour is achieved by the proposed distributed controller for voltage regulation, as shown in FIGURE 21. From FIGURE 20 and FIGURE 21, it is concluded that both the sharing of unbalanced-currents and the voltage regulation are achieved effectively by the proposed control scheme. Moreover, there is virtually no coupling between the proposed consensus controllers [(11) and (13)]. This is an important result since as was discussed in section II-A, the unbalanced-current control method (managed by $\beta_{ia}$, $\beta_{ib}$, $\beta_{ic}$) could interfere with the proposed voltage regulation controller, as is depicted by (9). This was overcome in this paper by setting (11) and (13) with different dynamic (by adjusting $k_i^u$ and $k_i^E$, respectively) as shown in TABLE 1. Therefore, it is demonstrated that the proposed consensus-based distributed algorithms (11) and (13) can achieve respectively, voltage regulation and the sharing of negative sequence current components, with virtually no coupling between them.

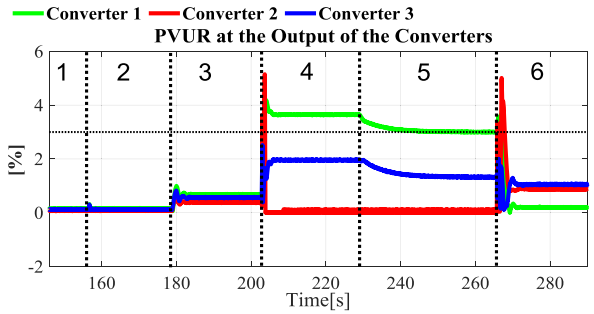


**FIGURE 22.** PVURs at the output of the converters in the six steps studied—MATLAB data logging of the experimental waveforms.

FIGURE 22 shows the PVUR at the output of each power converter in the six steps studied. This figure shows that in step 4 (when converter 2 is disconnected), the PVUR in converter 1 is 3.85%, i.e., over 3% (the maximum PVUR considered in this work). In step 5, the control terms to PVUR regulation are enabled [the first terms on the right-hand side of (11)], with a $PVUR_i^* = 3\%$, therefore, the PVUR in converter 1 is now effectively limited at 3%.

Finally, in FIGURE 23, the active powers injected by the converters into the MG, during this test are shown. As depicted in the figure, the proposed control scheme does not affect the injection of active power from the power converters to the MG.

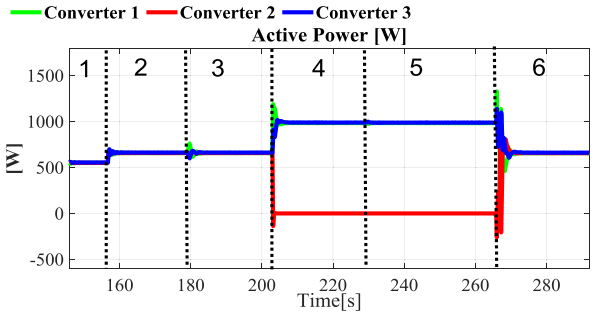


**FIGURE 23.** Active power at the output of the converters in the 6 steps studied —MATLAB data logging of the experimental waveforms.

### C. TEST SCENARIO 3: COMMUNICATION LINK FAILURE

In this test, the performance of the proposed control scheme for a communication fail in converter 2 is evaluated (see FIGURE 6 and FIGURE 14). Five steps are considered in this experimental test: in step 1, the proposed control scheme is disabled; in step 2, the control actions to regulate the voltage at the output of the power converters at 120V RMS are enabled. In step 3, the distributed control systems for unbalanced-current sharing are enabled. At the beginning of step 4 (and onwards), a communication failure between converter 1 and converter 2 is produced, setting the parameters of the adjacency matrix $a_{12}$ and $a_{21}$ equal to zero (see (15) and FIGURE 6). Finally, at the beginning of step 5, an additional

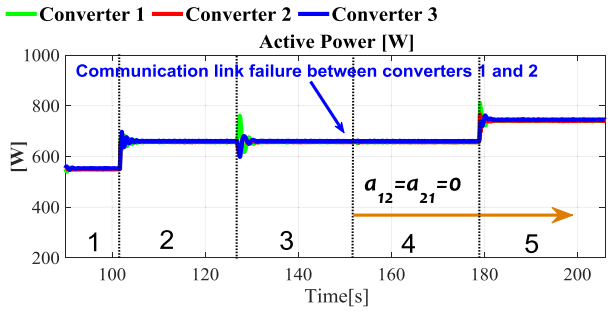


**FIGURE 24.** Active power at the output of the converters—MATLAB data logging of the experimental waveforms.

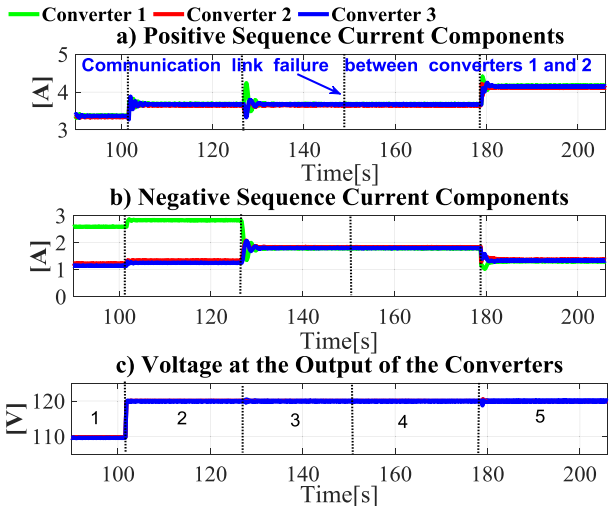


**FIGURE 25.** (a)-(b) Positive and negative sequence components of current at the output of power converters, (c) the average of the RMS voltage in the three phases of each power converter.

unbalanced load is connected, by closing the switch "$sw_4$" shown in FIGURE 6.

FIGURE 24 shows the active power inject by the converters to the MG. From this figure, it is concluded that the converters continue sharing active power despite the communication failure between converter 1 and converter 2. The same occurs with the positive and negative sequence components of the current at the output of converters [see FIGURE 25(a)-(b)], and with the voltage at their outputs [see FIGURE 25(c)]. A significant result from FIGURE 24 and FIGURE 25 is the fact that the proposed methodology for sharing unbalanced-currents and voltage regulation operates well even when a communication failure is produced. It should be highlighted that FIGURE 25(a)-(b) were obtained by applying the SCT to the experimental waveforms. From these figures, it can be concluded that the proposed single-phase approach for unbalanced-current sharing (11), effectively achieves the sharing of negative sequence current components among the power converters. In other words, it is demonstrated that the proposed single-phase approach is an effective way of controlling negative sequence components without the need for implementing sequence separation

algorithms, and thus, avoiding all the drawbacks associated with them. (Noise, harmonic distortion, variations in the sampling time magnitude, etc. [28])

## V. CONCLUSION

A consensus-based distributed control scheme for the sharing of unbalanced-currents and voltage regulation in isolated 3-wire AC MGs have been proposed in this work. The proposed consensus algorithm achieves the sharing of negative sequence current components among the power converters without the need to implement the SCT or the CPT (some of the typical solution for dealing with this problem). Moreover, the proposed distributed scheme does not interfere with the sharing of active power between the power converters, evidencing its decoupled performance.

The main advantages of the proposal over other reported distributed controllers for imbalance sharing [24]–[26] are: (i) the proposed control scheme achieves the sharing of unbalanced currents producing smaller imbalances in the converters' output voltages compared with other methods, and (ii) the proposal achieves sharing of unbalanced currents in both the sequence domain and the a-b-c domain. The latter is difficult to realise using previously reported methods, as was demonstrated in section III-A.

From the experimental validation, the following conclusions are derived:

(i) The performance of the proposed method can react effectively to load changes. When a load change is imposed (see section IV-A), both the correct sharing of unbalanced currents and correct voltage regulation are maintained.

(ii) The plug and play capability of the proposal was demonstrated in the experimental test depicted in section IV-B. During this test, the disconnection and subsequent reconnection of converter 2 is emulated with the experimental MG of FIGURE 14. During this critical scenario, it is appreciated that the proposed control scheme maintains proper voltage regulation and sharing of unbalanced-current, validating the effectiveness of the proposal.

(iii) The performance of the distributed control scheme in the presence of communication failures was evaluated in Section IV-C by emulating communication failure between converter 1 and converter 2 (FIGURE 14). From this experimental test, it is concluded that the control objectives continue to be achieved even in this extreme situation.

As future work, the extension of the proposed distributed control scheme to 4-wire AC MGs will be addressed. The application of the proposed control methodology for sharing of distorted currents produced by nonlinear loads will also be studied and reported in a future publication. Finally, the extension of the proposal to a multi-microgrid system will be studied further.

## REFERENCES

[1] M. Hamzeh, S. Emamian, H. Karimi, and J. Mahseredjian, "Robust control of an islanded microgrid under unbalanced and nonlinear load conditions," *IEEE J. Emerg. Sel. Topics Power Electron.*, vol. 4, no. 2, pp. 512–520, Jun. 2016.

[2] D. Sreenivasarao, P. Agarwal, and B. Das, "Neutral current compensation in three-phase, four-wire systems: A review," *Electr. Power Syst. Res.*, vol. 86, pp. 170–180, May 2012.

[3] S. P. Oe, E. Christopher, M. Sumner, S. Pholboon, M. Johnson, and S. A. Norman, "Microgrid unbalance compensator-Mitigating the negative effects of unbalanced microgrid operation," in *Proc. IEEE PES ISGT Eur.*, Lyngby, Denmark, Oct. 2013, pp. 1–5.

[4] E. Nasr-Azadani, C. A. Cañizares, D. E. Olivares, and K. Bhattacharya, "Stability analysis of unbalanced distribution systems with synchronous machine and DFIG based distributed generators," *IEEE Trans. Smart Grid*, vol. 5, no. 5, pp. 2326–2338, Sep. 2014.

[5] R. H. Salim, R. A. Ramos, and N. G. Bretas, "Analysis of the small signal dynamic performance of synchronous generators under unbalanced operating conditions," in *Proc. IEEE PES Gen. Meeting*, Providence, RI, USA, Jul. 2010, pp. 1–6.

[6] M. Savaghebi, A. Jalilian, J. C. Vasquez, and J. M. Guerrero, "Secondary control for voltage quality enhancement in microgrids," *IEEE Trans. Smart Grid*, vol. 3, no. 4, pp. 1893–1902, Dec. 2012.

[7] L. Meng, F. Tang, M. Savaghebi, J. C. Vasquez, and J. M. Guerrero, "Tertiary control of voltage unbalance compensation for optimal power quality in islanded microgrids," *IEEE Trans. Energy Convers.*, vol. 29, no. 4, pp. 802–815, Dec. 2014.

[8] C. Burgos-Mellado, R. Cardenas, D. Saez, A. Costabeber, and M. Sumner, "A control algorithm based on the conservative power theory for cooperative sharing of imbalances in four-wire systems," *IEEE Trans. Power Electron.*, vol. 34, no. 6, pp. 5325–5339, Jun. 2019.

[9] *IEEE Standard for Interconnection and Interoperability of Distributed Energy Resources With Associated Electric Power Systems Interfaces*, document I. S. 1547-2018, 2018.

[10] E. Espina, R. Cárdenas-Dobson, M. Espinoza-B, C. Burgos-Mellado, and D. Saez, "Cooperative regulation of imbalances in three-phase four-wire microgrids using single-phase droop control and secondary control algorithms," *IEEE Trans. Power Electron.*, vol. 35, no. 2, pp. 1978–1992, Feb. 2020.

[11] X. Zhou, F. Tang, P. C. Loh, X. Jin, and W. Cao, "Four-leg converters with improved common current sharing and selective voltage-quality enhancement for islanded microgrids," *IEEE Trans. Power Del.*, vol. 31, no. 2, pp. 522–531, Apr. 2016.

[12] X. Feng, A. Shekhar, F. Yang, R. E. Hebner, and P. Bauer, "Comparison of hierarchical control and distributed control for microgrid," *Electr. Power Compon. Syst.*, vol. 45, no. 10, pp. 1043–1056, Jun. 2017.

[13] F. Guo, C. Wen, J. Mao, and Y.-D. Song, "Distributed economic dispatch for smart grids with random wind power," *IEEE Trans. Smart Grid*, vol. 7, no. 3, pp. 1572–1583, May 2016.

[14] G. Binetti, A. Davoudi, F. L. Lewis, D. Naso, and B. Turchiano, "Distributed consensus-based economic dispatch with transmission losses," *IEEE Trans. Power Syst.*, vol. 29, no. 4, pp. 1711–1720, Jul. 2014.

[15] G. Chen and Z. Guo, "Distributed secondary and optimal active power sharing control for islanded microgrids with communication delays," *IEEE Trans. Smart Grid*, vol. 10, no. 2, pp. 2002–2014, Mar. 2019.

[16] Q. Shafiee, J. M. Guerrero, and J. C. Vasquez, "Distributed secondary control for islanded microgrids—A novel approach," *IEEE Trans. Power Electron.*, vol. 29, no. 2, pp. 1018–1031, Feb. 2014.

[17] J. W. Simpson-Porco, Q. Shafiee, F. Dörfler, J. C. Vasquez, J. M. Guerrero, and F. Bullo, "Secondary frequency and voltage control of islanded microgrids via distributed averaging," *IEEE Trans. Ind. Electron.*, vol. 62, no. 11, pp. 7025–7038, Nov. 2015.

[18] L.-Y. Lu and C.-C. Chu, "Consensus-based secondary frequency and voltage droop control of virtual synchronous generators for isolated AC micro-grids," *IEEE J. Emerg. Sel. Topics Circuits Syst.*, vol. 5, no. 3, pp. 443–455, Sep. 2015.

[19] R. Han, L. Meng, G. Ferrari-Trecate, E. A. A. Coelho, J. C. Vasquez, and J. M. Guerrero, "Containment and consensus-based distributed coordination control to achieve bounded voltage and precise reactive power sharing in islanded AC microgrids," *IEEE Trans. Ind. Appl.*, vol. 53, no. 6, pp. 5187–5199, Nov. 2017.

[20] J. Lai, X. Lu, X. Li, and R.-L. Tang, "Distributed multiagent-oriented average control for voltage restoration and reactive power sharing of autonomous microgrids," *IEEE Access*, vol. 6, pp. 25551–25561, 2018.

[21] J. Llanos, D. E. Olivares, J. W. Simpson-Porco, M. Kazerani, and D. Saez, "A novel distributed control strategy for optimal dispatch of isolated microgrids considering congestion," *IEEE Trans. Smart Grid*, vol. 10, no. 6, pp. 6595–6606, Nov. 2019.

[22] J. S. Gomez, D. Saez, J. W. Simpson-Porco, and R. Cardenas, "Distributed predictive control for frequency and voltage regulation in microgrids," *IEEE Trans. Smart Grid*, vol. 11, no. 2, pp. 1319–1329, Mar. 2020.
[23] G. Lou, W. Gu, W. Sheng, X. Song, and F. Gao, "Distributed model predictive secondary voltage control of islanded microgrids with feedback linearization," *IEEE Access*, vol. 6, pp. 50169–50178, 2018.
[24] L. Meng, X. Zhao, F. Tang, M. Savaghebi, T. Dragicevic, J. C. Vasquez, and J. M. Guerrero, "Distributed voltage unbalance compensation in islanded microgrids by using a dynamic consensus algorithm," *IEEE Trans. Power Electron.*, vol. 31, no. 1, pp. 827–838, Jan. 2016.
[25] J. Zhou, S. Kim, H. Zhang, Q. Sun, and R. Han, "Consensus-based distributed control for accurate reactive, harmonic, and imbalance power sharing in microgrids," *IEEE Trans. Smart Grid*, vol. 9, no. 4, pp. 2453–2467, Jul. 2018.
[26] C. Burgos-Mellado, J. J. Llanos, R. Cardenas, D. Saez, D. E. Olivares, M. Sumner, and A. Costabeber, "Distributed control strategy based on a consensus algorithm and on the conservative power theory for imbalance and harmonic sharing in 4-wire microgrids," *IEEE Trans. Smart Grid*, vol. 11, no. 2, pp. 1604–1619, Mar. 2020.
[27] X. Wu, C. Shen, and R. Iravani, "Feasible range and optimal value of the virtual impedance for droop-based control of microgrids," *IEEE Trans. Smart Grid*, vol. 8, no. 3, pp. 1242–1251, May 2017.
[28] J. Svensson, M. Bongiorno, and A. Sannino, "Practical implementation of delayed signal cancellation method for phase-sequence separation," *IEEE Trans. Power Del.*, vol. 22, no. 1, pp. 18–26, Jan. 2007.
[29] J. Guo, K. Ren, X. Yang, J. Si, P. Yue, and R. Khan, "Improved park inverse transform algorithm for positive and negative sequence separation of grid voltage under unbalanced grid conditions," in *Proc. Chin. Control Conf. (CCC)*, Guangzhou, China, Jul. 2019, pp. 7256–7262.
[30] C. B. Mellado, "Control strategies for improving power quality and PLL stability evaluation in microgrids," Ph.D. dissertation, Dept. Elect. Electron. Eng., Univ. Nottingham, Nottingham, U.K., 2018.
[31] C. Burgos-Mellado, C. Hernández-Carimán, R. Cardenas, D. Saez, M. Sumner, A. Costabeber, and H. K. M. Paredes, "Experimental evaluation of a CPT-based four-leg active power compensator for distributed generation," *IEEE J. Emerg. Sel. Topics Power Electron.*, vol. 5, no. 2, pp. 747–759, Jun. 2017.
[32] X. Wu, Y. Xu, J. He, C. Shen, G. Chen, J. C. Vasquez, and J. M. Guerrero, "Delay-dependent small-signal stability analysis and compensation method for distributed secondary control of microgrids," *IEEE Access*, vol. 7, pp. 170919–170935, 2019.
[33] X. Chen, M. Shi, H. Sun, Y. Li, and H. He, "Distributed cooperative control and stability analysis of multiple DC electric springs in a DC microgrid," *IEEE Trans. Ind. Electron.*, vol. 65, no. 7, pp. 5611–5622, Jul. 2018.
[34] Y. Yan, D. Shi, D. Bian, B. Huang, Z. Yi, and Z. Wang, "Small-signal stability analysis and performance evaluation of microgrids under distributed control," *IEEE Trans. Smart Grid*, vol. 10, no. 5, pp. 4848–4858, Sep. 2019.

**CLAUDIO BURGOS-MELLADO** (Member, IEEE) was born in Cunco, Chile. He received the B.Sc. and M.Sc. degrees in electrical engineering from the University of Chile, Santiago, Chile, in 2012 and 2013, respectively, the Ph.D. degree in electrical and electronic engineering from the University of Nottingham, U.K., and the Ph.D. degree in electrical engineering from the University of Chile, in 2019. He is currently a Research Fellow with the Power Electronics, Machines and Control Group (PEMC Group), University of Nottingham. His current research interests include battery energy storage systems, electrical vehicle technologies, power electronics, microgrids, and power quality.

**JACQUELINE LLANOS** (Member, IEEE) received the B.Sc. and Engineering degrees in electronic engineering from the Army Polytechnic School, Ecuador, and the M.Sc. degree in electrical engineering from the University of Chile, Santiago, where she is currently pursuing the Ph.D. degree. She is also an Assistant Professor with the Department of Electrical and Electronic, Universidad de las Fuerzas Armadas ESPE, Ecuador. Her current research interests include control and management of microgrids, control of power generation plants, and predictive control.

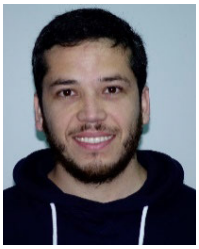

**ENRIQUE ESPINA** (Graduate Student Member, IEEE) was born in Santiago, Chile. He received the B.Sc. degree in electrical engineering from the University of Santiago, Chile, in 2013, and the M.Sc. degree in electrical engineering from the University of Chile, in 2017. He is currently pursuing the double Ph.D. degrees in electrical engineering with the University of Chile and the University of Waterloo, Canada. His main research interests include control of hybrid microgrids, renewable energies, and power electronic converters.

**DORIS SÁEZ** (Senior Member, IEEE) was born in Panguipulli, Chile. She received the M.Sc. and Ph.D. degrees in electrical engineering from the Pontificia Universidad Católica de Chile, Santiago, Chile, in 1995 and 2000, respectively. She is currently a Full Professor with the Department of Electrical Engineering and the Head of the Indigenous People Program, Faculty of Mathematical and Physical Sciences, University of Chile, Santiago. She has coauthored the books *Hybrid Predictive Control for Dynamic Transport Problems* (Springer Verlag, 2013) and *Optimization of Industrial Processes at Supervisory Level: Application to Control of Thermal Power Plants* (Springer-Verlag, 2002). Her research interests include predictive control, fuzzy control design, fuzzy identification, and control of microgrids. She serves as an Associate Editor for the IEEE TRANSACTIONS ON SMART GRID.

**ROBERTO CÁRDENAS** (Senior Member, IEEE) was born in Punta Arenas, Chile. He received the B.S. degree from the University of Magallanes, Chile, in 1988, and the M.Sc. and Ph.D. degrees from the University of Nottingham, U.K., in 1992 and 1996, respectively. From 1989 to 1991 and from 1996 to 2008, he was a Lecturer with the University of Magallanes. From 1991 to 1996, he was also with the Power Electronics Machines and Control Group (PEMC Group), University of Nottingham. He is currently a Full Professor of power electronics and drives with the Electrical Engineering Department, University of Chile, Chile. His main research interests include control of electrical machines, variable speed drives, and renewable energy systems.

**MARK SUMNER** (Senior Member, IEEE) received the B.Eng. degree in electrical and electronic engineering from the University of Leeds, in 1986, and the Ph.D. degree in induction motor drives from the University of Nottingham, U.K., in 1990. He was with Rolls Royce Ltd., U.K. He was also a Research Assistant and a Lecturer in October 1992. He is currently a Professor of electrical energy systems with the Power Electronics, Machines and Control Group (PEMC Group), University of Nottingham. His research interests include control of power electronic systems, including sensorless motor drives, diagnostics and prognostics for drive systems, power electronics for enhanced power quality, and novel power system fault location strategies.

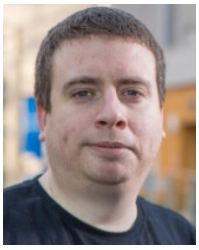

**ALAN WATSON** (Member, IEEE) received the M.Eng. degree (Hons.) in electronic engineering and the Ph.D. degree from the University of Nottingham, U.K., in 2004 and 2008, respectively. In 2009, he was a Research Fellow with the Power Electronics Machines and Control Group, University of Nottingham. Since 2009, he has been involved in various projects in high-power electronics, including resonant converters, high-voltage power supplies, and multilevel converters for grid connected applications, such as HVDC and flexible AC transmission systems. In 2012, he was a Senior Research Fellow. He is currently an Assistant Professor in high power electronics with the Power Electronics, Machines and Control Group (PEMC Group), University of Nottingham. His current research interests include development and control of advanced high-power conversion topologies for industrial applications, grid connected converters, and HVDC transmission.